2019

# Fabrication of Polyelectrolyte Nanoparticles Through Hydrophobic Interaction

Ruginn Porce Catarata
*University of Central Florida*

# FABRICATION OF POLYELECTROLYTE NANOPARTICLES THROUGH HYDROPHOBIC INTERACTIONS

by

RUGINN CATARATA
B.S. University of Central Florida, 2015

A thesis submitted in partial fulfillment of the requirements
for the degree of Master of Science
in the NanoScience Technology Center
in the College of Graduate Studies
at the University of Central Florida
Orlando, Florida

Fall Term
2019

Major Professor: Lei Zhai

# ABSTRACT

Anticancer drugs like gemcitabine (GEM) are used to treat cancers such as, pancreatic ductal adenocarcinoma (PDAC). However, the use of free gemcitabine yields challenges including cytotoxicity to healthy cells and poor circulation time. By encapsulating GEM in nanoparticles these challenges can be overcome. In this study poly(acrylic acid) (PAA)-GEM nanoparticles are fabricated by coupling GEM onto PAA. The particle formation is driven by the hydrophobic interaction of GEM, which collects in the core of the nanoparticle, forming a PAA shell. The nanoparticles were optimized by studying the PAA/GEM ratio and pH during fabrication. Characteristics of the nanoparticles including size, morphology and surface charge were investigated using dynamic light scattering (DLS), transmission electron microscopy (TEM) and zeta potential measurements. Conditions such as ionic stability and pH stability were optimized to achieve high drug loading efficiency. Cell uptake and cytotoxicity studies were used to determine the efficiency of the nanoparticles as drug delivery vehicle.



*Keywords:* Nanoparticles, polyelectrolytes, hydrogel, drug delivery, pancreatic cancer

# ACKNOWLEDGEMENTS

There are many people that I must thank when I think about my time at the Nanoscience Technology Center. Firstly, I must thank Dr. Lei Zhai for giving me the incredible opportunity to join his group during my undergraduate career, a gift that I am forever grateful for. His teachings and guidance throughout this mentorship are things that will continue to practice throughout my life. I must also thank the rest of my committee members Dr. Ellen Hyeran Kang and Dr. Qun "Treen" Huo for their support and reassurance during this journey. Thank you to Dr. Santanu Bhattacharya, our collaborator at Mayo Clinic, thank you for your continued support and patience during our collaboration.

I could not have accomplished anything without the teachings, outings, and discussions with my lab members. It has been a pleasure to come in and work with such brilliant and creative minds. Each of you have a place in my heart and have made this portion of my life enjoyable and memorable.

I am grateful to the Mayo-UCF award and the National Science Foundation for support in the projects. Lastly, I must thank my family for without their sacrifice and support I would not be strong enough to continue. Thank you

# TABLE OF CONTENTS

# LIST OF FIGURES

# LIST OF TABLES

# LIST OF ACRONYMS (or) ABBREVIATIONS

| | |
|---|---|
| 3D | Three-Dimensional |
| DLS | Dynamic Light Scatter |
| DMEM | Dulbecco's Modified Eagle Medium |
| DNA | Deoxyribonucleic Acid |
| EDC | 1-Ethyl-3-(3-dimethylaminopropyl) carbodiimide |
| FT-IR | Fourier Transform Infrared Spectroscopy |
| GEM | Gemcitabine |
| NaOH | Sodium Hydroxide |
| PAA | Polyacrylic(acid) |
| PBS | Phosphate Buffer Saline |
| PC | Pancreatic Cancer |
| PDAC | Pancreatic Ductal Adenocarcinoma |
| RG6 | Rhodamine G6 |
| TEM | Transmission Electron Microscopy |

# CHAPTER ONE: INTRODUCTION

## Polymeric Nanoparticles

With the eruption of nanotechnology and their many applications, the focus on nanomaterials has increased in the last few decades.[1, 2] Platforms such as nanoparticles which range from a few nanometers to 100 nm, have shown great promise because of their surface area to volume ratio compared to bulk materials. [1-4] As a result of their physical and chemical characteristics, nanoparticles are effective in applications such as drug delivery[3], antimicrobial interactions[5], catalysis[6], energy storage[7]. A wide variety of nanoparticles are used, including metals[8], quantum dots[9], liposomes[10] and polymeric[11] nanoparticles and they all present some advantages and shortcomings.

Important factors to consider when fabricating nanoparticles are the size and surface chemistry of the nanoparticles. Using polymers for nanoparticle fabrication allows for tunable characteristics that rely on the fabrication method of the nanoparticle and the polymers used.[12, 13] Natural and synthetic polymers have been used in the formation of polymeric nanoparticles. Natural polymers have been noted to form more polydispersed particles from each batch. In contrast, synthetic polymers have been seen to have more controlled size.[12] One of the major advantages of using polymers as the platform for nanoparticle is the biocompatibility and biodegradability of some natural and synthetic polymers..[12, 14]

### *Hydrogel Nanoparticles*

Hydrogels are a three-dimensional (3D) network of crosslinked hydrophilic polymers that can uptake and retain large amounts of fluids without dissolving.[15, 16] Their ability to retain fluids is a result of different functional groups on the polymers such as -OH, -CONH-, -$CONH_2$- and -

$SO_3H$. These different functional groups within the polymer network also allow the hydrogel to swell and de-swell by uptaking and releasing fluid based on the environment of the hydrogel. [3, 16] The degree of crosslinking within the hydrogel allows for the resistance in degradation.[16] Physical hydrogels and chemical hydrogels are categories of hydrogels that are based on the method at which crosslinking happens. Physical crosslinking occurs via intermolecular forces such as hydrogen bonding, van der Waals interaction and ion dipole.[3] Chemical crosslinked hydrogels are formed by covalent bonds between different functional groups within a polymer. [17]

Hydrogel nanoparticles share the unique properties of both nanoparticles and hydrogels. Hydrogels have similar properties to living tissue as they share a similar consistency, elasticity, fluid content and porosity.[18, 19] As a result, they are ideal candidates for biomedical applications such as tissue engineering[20], drug delivery[21], wound healing[22], injectable fillers[23], and biosensors.[24]

## Drug Delivery Platforms

As previously mentioned, polymeric nanoparticles serve as an optimal candidate for drug delivery platforms because of their biocompatibility, biodegradability and their tunable characteristics.[12, 13] Additionally, the nanoparticle allows for improved drug efficacy and protection of the drug from chemical degradation.[3] In the case of hydrogel nanoparticles, the polymers can be highly functionalized based on the surface of the nanoparticle and they exhibit an excellent drug released mechanism as a result of their swelling and deswelling properties.[25] Nanoparticles can also serve as targeting vehicle for drug delivery as they can be decorated with targeting enzymes to select for specific cell types. [26, 27] Nanoparticles for drug delivery can exist either as nanocapsules or nanospheres depending on the fabrication of the nanoparticle. Nanocapsules are hollow nanoparticles in which the drug can be confined within the center of the

nanoparticle. Nanospheres are solid uniformly crosslinked particles where the drug is evenly distributed within the particle.[3, 14]

## Fabrication of Polymeric Nanoparticles

The method by which nanoparticles are fabricated directly affects their size, morphology and monodispersity, making this area of research very important for downstream applications of the nanoparticles.[1] There are numerous approaches for the fabrication of polymeric nanoparticles including, emulsion[28], dendrimers[29], and precipitation.[30]

In an emulsion, a micelle can be formed to act as templates for the fabrication of polymer nanoparticles. This type of nanoparticle is fabricated using a small molecule that contains a hydrophobic and hydrophilic end called an amphiphilic molecule or a surfactant.[31] In the traditional formation of a micelle there are two phases, a water phase and an oil phase, with the water phase being larger. The amphiphilic molecule will interact with both phases upon agitation and nanoparticles will form. The nanoparticle will contain an exterior hydrophilic phase and an internal hydrophobic phase and the formation of the particle is due to the hydrophobic and hydrophilic interactions of the surfactant and the solvent phase.[32-34] In a reverse emulsion the micelle will have an exterior hydrophobic phase and an internal hydrophilic phase.[28] However, the emulsion method for nanoparticle fabrication can result in non-biocompatible by-products and multiple purification steps may be required.[12]

Dendrimers are a type of polymer nanoparticles formed from hyperbranched polymerization.[29, 35] A dendrimer is composed of an atom or a collection of atoms called the core, and the branches are referred to as the dendrons.[35] Dendrimers can be formed by two approaches:

divergent and convergent.[36] The divergent formation of dendrimers begins with the core, which then grows outwards by reacting with a monomer consisting of three groups, a reactive group and two dormant groups. The polymerization continues in a step by step manner with more monomer.[35] In contrast, the convergent approach begins with the most exterior branches and grows inwards, this results in the predetermined size.[36] However, the fabrication is time consuming and requires multistep synthesis.[35]

Nanoprecipitation or solvent displacement is another method to fabricate polymers nanoparticles. [12, 37] In this method the nanoparticles are formed from the addition of two miscible solvents (solvent and non-solvent) and magnetic stirring, resulting in immediate formation of nanoparticles after phase separation.[37-39] Typically the polymer and the drug will be in the solvent phase.[39] The formation is due to interfacial deposition after the polymer is displaced from the solvent phase into the non-solvent phase.[12, 37] This method of fabrication is typically easier than the formation of polymer nanoparticles through emulsion because of its simplicity and lack of toxic solvents.[37]

Block polymers are also used in the fabrication of polymeric nanoparticles where the block polymer consists of two different polymers with different properties. One example of such nanoparticle is composed of two polymers, one bearing a hydrophobic region and the other a hydrophilic region. Based on hydrophobic interactions of the polymer and the solvent the block polymer is formed.[40]

## Focus of Research

Currently, pancreatic cancer is the fourth cause of cancer related deaths and is predicted to become the second position by 2030. This is a result of the difficultly of treatment and early diagnosis of pancreatic cancer. The 5-year survival rate for pancreatic cancer is only 5%, with 80% of diagnosed patients anticipated to die within 12 months. The lack of distinctive side effects of pancreatic cancer results in diagnosis at later stages of the disease, this leads to difficulty in treatment. Pancreatic ductal adenocarcinoma (PDAC) is the most common type of pancreatic cancer consuming > 90% of pancreatic cancer types. PDAC is also the most demanding in regards to treatment.[41] The current treatment methods for PC are futile and better treatment methods are needed in order to better treat the cancer.

The first line of defense to treat pancreatic cancer is gemcitabine (2',2'-difluro-2'-deoxycytidine) (GEM), an anticancer chemotherapy. GEM is analog to the DNA base deoxycytidine and inhibits DNA synthesis, resulting in apoptosis of cells (Figure 1).[42] However, gemcitabine has a short plasma half-life and is quickly metabolized by cytidine deaminase into a non-active form.[43] As a result, high concentration of GEM is needed for treatment. An alternative approach with the protection of GEM can also be investigated.

Nanotechnologies, such as the use of nanoparticles, serve as delivery systems that can be used to protect the drug of interest and also allow multiple modalities to the system such as fluorescence and targeting.[26, 27] Several studies have already fabricated gemcitabine loaded nanoparticles with great success.[44-46] However, none have driven the formation of the particle from the hydrophobic regions of gemcitabine.

Here, we use poly(acrylic acid) (PAA) a biodegradable and biocompatible polymer for the formation of nanoparticles.[47, 48] The fabrication of the PAA-GEM nanoparticles are achieved through hydrophobic interactions from the fluorine atoms in GEM. The characteristics including size, surface charge and stability were investigated. The in vitro release of drug, cell toxicity and cell uptake of the nanoparticle were also investigated.

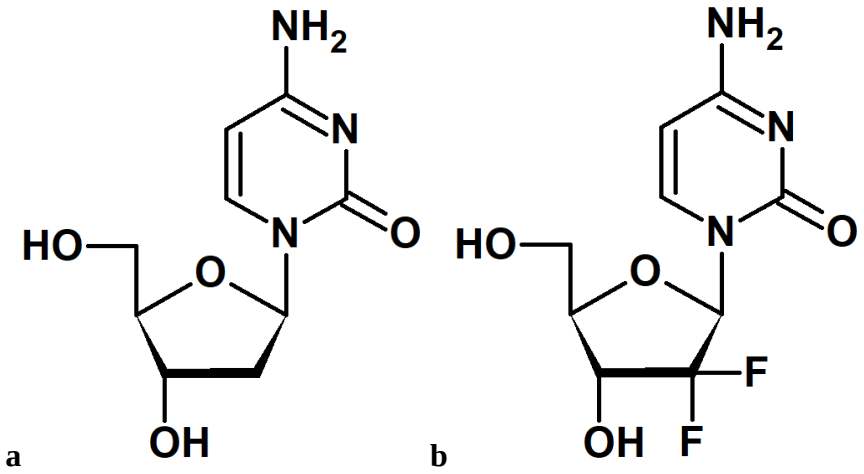


Figure 1 Structure of deoxycytidine (a) and gemcitabine (b)

# CHAPTER TWO: MATERIALS AND METHODS

## Materials

Poly(acrylic acid) partial sodium salt solution (~240,000 Da, 25%), anhydrous sodium acetate and rhodamine G6 (95%) was purchased from Sigma Aldrich. Gemcitabine (98%) and acetic acid was purchased from Acros Organic, Sodium hydroxide was purchased from Fisher Chemical. 1-Ethyl-3-(3-dimethylaminopropyl) carbodiimine (EDC) was purchased from Oakwood Chemical. PBS was purchased from Corning Cellgro. Fetal Bovine Serum (FBS), Penicillin Streptomycin and Dulbecco's Modified Eagle Medium (DMEM) was purchased from Life Technologies-ThermoFisher Scientific. PANC-1 cells were obtained from American Type Culture Collection (ATCC).

## Nanoparticle Fabrication

The fabrication of PAA-GEM nanoparticles is as followed, GEM was dissolved in a solution of 10 mg/mL PAA for molar ratios of 1:2, 1:4, 1:8 and 1:16. Each solution was then adjusted to pH 4 with 1 M NaOH. In each sample a specific amount of 1-ethyl-3-(3-dimethylaminopropyl) carbodiimide hydrochloride (EDC) was added, the solution was stirred overnight via magnetic stirring at ambient conditions. The above solutions were then purified via centrifugation at 110,000 rpm for 60 minutes at 4 °C via ultra-centrifugate (Sorvall MTX 150 Micro Ultracentrifuge, Thermo Scientific). The supernatant was collected for UV-analysis. The pellet was resuspended with water, loaded into dialysis tubing (MWCO 12-14 kDa, SpectraPor) and underwent 3 phases dialysis until the full removal of free GEM, EDC and EDC by-product. The dialysis product was then frozen and lyophilized.

## Encapsulation Efficiency and Loading Capacity:

The supernatant collected was then measured through UV-vis spectroscopy (Cary 300 Bio UV-Visible Spectrophotometer) for analysis of the gemcitabine at the wavelength of 268 nm. The collected sample was compared against calibrated standards. The following formulas were used to calculate the encapsulation efficiency (EE) and loading capacity (LC):

$$EE = \frac{(\text{Total amount of drug added} - \text{Free amount of drug})}{\text{Total amount of drug}} * 100 \quad (1)$$

$$LC = \frac{(\text{Total amount of drug} - \text{Free amount of drug})}{\text{Total weight of lyophilized nanoparticles}} * 100 \quad (2)$$

## Nanoparticle Decoration: Rhodamine G6

The lyophilized sample of nanoparticles were resuspended with deionized water (3 mg/mL) and were bath sonicated for 5 minutes. Under magnetic stirring, 1 mg/mL Rhodamine G6 (RG6) was introduced to the nanoparticles for a 10,000:1 molar ratio between PAA:RG6. EDC was added to the solution at a 1:1 molar ratio between EDC:RG6. The solution was then purified following the same protocol as for pristine PAA-GEM nanoparticles.

## Nanoparticle Characterization

At various steps of nanoparticle fabrication, the size and surface charge were characterized by dynamic light scatter and zeta potential (Malvern Zetasizer, Nano ZS90). The nanoparticles were examined after initial fabrication and after resuspension in various solvents. The morphology of the nanoparticles were examined via transmission electron microscopy (TEM) (JEOL TEM-1011). Chemical characteristics of the PAA-GEM nanoparticle were determined through Fourier

transform infrared spectroscopy (FT-IR) (Perkin Elmer Spectrum 100) and compared against PAA and GEM.

## Nanoparticle Stability

The stability of the nanoparticles was determined by analyzing the size and surface charge of the nanoparticles for 7 days in different pH environments. Lyophilized samples of PAA-GEM nanoparticles were resuspended in sodium acetate buffer (pH 3, 4, 5, 6) and phosphate buffer saline (PBS) at pH 7.4 at a concentration of 3 mg/mL.

## In Vitro Drug Release

The release profile of PAA-GEM nanoparticles was investigated, 100 mg of lyophilized nanoparticle sample was resuspended in 20 mL of PBS and placed in dialysis bags (MWCO 12-14 kDa, SpectraPor). The same amount of free GEM was dissolved 20 mL PBS and placed in dialysis bags. The samples underwent dialysis against 80 mL of PBS in closed containers at ambient conditions with slight agitation via mechanical stirring. At various time intervals 3 mL of releasing phase was collected and replaced with 3 mL of fresh PBS. The collected aliquots were analyzed through UV-spectroscopy at 268 nm and compared against calibrated solutions.

## Cytotoxicity Study

Approximately 5000 PANC-1 cells were seeded in each well of 96-well plates and cultured in Dulbecco's modified Eagle medium (DMEM) supplemented with 10% fetal bovine serum (FBS) and 1% penicillin-streptomycin. Cells were cultured at 37 °C in a humidified 5% carbon dioxide atmosphere. After overnight cell culture, cells were treated with PAA-GEM nanoparticles

and equivalent controls at various concentrations for 24, 48, 72 and 96 hours time points. At each time point cells were thoroughly washed with PBS. Cell viability assay was conducted using "Celltiter 96 Aqueous One Solution Cell Proliferation Assay" as per the manufacturer's protocol. Briefly, 20 µL of the reagent was be added to each well of 96-well plates containing 100 µL of complete culture medium, and the plate was incubated at 37 ℃ for 1-4 hours. Absorbance at 490 nm was be measured and plotted against respective time points to obtain a viability curve

## Nanoparticle Cellular Uptake

PAA-GEM-RG6 nanoparticles were analyzed for the uptake within PANC-1 cells. PANC-1 cells were treated with PAA-GEM-RG6 nanoparticles at various times: 30 minutes, 1 hour, 2 hours, 3 hours, 4 hours, 5 hours, and 6 hours. At the end of the incubation time the cells were washed with PBS and replaced with clean media. The cells were observed by optical microscopy for the analysis of nanoparticle uptake.

# CHAPTER THREE: RESULTS

Nanoparticle Fabrication:

The PAA:GEM ratios were investigated for the fabrication of nanoparticles. Table 1 demonstrates, the effect of different PAA:GEM molar ratios 2:1, 4:1, 8:1 and 16:1 on the nanoparticles being formed. The 8:1 and 16:1 PAA:GEM solutions resulted in clear solutions, indicating no nanoparticles were formed. In contrast, the 2:1 solution created a cloudy agglomeration of particles with a size range of 3574 ± 493.1 nm, a PDI (polydispersity index) of 0.264 ± 0.133 and a zeta potential of -23.0 ± 4.42 mV. The 4:1 ratio resulted in an opalescent solution with monodispersed particles at 69.62 ± 0.419 nm, a PDI of 0.211 ± 0.014 and a zeta potential of -16.8 ± 1.36 mV.

The effect of EDC:GEM was investigated for the 4:1 and the 8:1 PAA:GEM ratios . As the concentration of EDC is increased for the 4:1 PAA:GEM samples, the solution became more cloudy and the size of the nanoparticles increased, resulting in micron sized particles for both the 4:1:4 and 4:1:8 (PAA:GEM:EDC), as shown in table 2. In addition, the PDI increased with the increased concentration of EDC, resulting in a more polydispersed mixture of nanoparticles. As previously recorded, the 8:1:2 (PAA:GEM) solution failed to form nanoparticles with a 2:1 EDC:GEM ratio. However, when increased the 4:1 and 8:1 EDC:GEM ratios were able to form nanoparticles. The 8:1:4 (PAA:GEM:EDC) solution formed 43.38 ± 7.635 nm particles, with a PDI of 0.401 ± 0.125 and a zeta potential of -16.5 ± 0.529 mV. Interestingly, the 8:1:8 (PAA:GEM:EDC) solution formed smaller nanoparticles at 28.74 ± 0.127 nm, with a PDI of 0.229 ± 0.006 and a zeta potential of -15.8 ± 0.802 mV.

## Nanoparticle Charaterization: Size, Morphology and Surface Charge

The sizes and surface charges of the nanoparticles were determined through dynamic light scattering and zeta potential in the previous section. The particles were measured in many states including after fabrication and after resuspension in PBS. The particles demonstrated a size of 28.74 ± 0.127 nm after fabrication at pH 4 and when resuspension in PBS the particles demonstrated a size of 57.84 ± 1.909 nm.

TEM was used to determine the size and morphology of the PAA:GEM nanoparticles. The nanoparticles demonstrated a spherical morphology with a size of 12.32 ± 1.96 nm, as shown in Figure 2a. Figure 2b shows a histogram of the size of the nanoparticles, revealing the monodispersed size of nanoparticles. Table 3 shows the size of PAA-GEM nanoparticles compared to PAA-GEM-RG6 nanoparticles. Rhodamine G6 attached particle demonstrates a slight increase in size as well as a more negative zeta potential than the nanoparticles without RG6.

## Gemcitabine to Poly(acrylic acid) Conjugation

In order to confirm the conjugation of GEM to PAA, FT-IR was used to determine if new bond formations had occurred. As gemcitabine was attached to PAA via EDC coupling the formation of an amide bond was the target. Figure 3, demonstrates the formation of an amide bond in the PAA-GEM samples with the C=O stretching at 1680-1700 $cm^{-1}$ as the amide I band. The amide II band at 1550-1510 $cm^{-1}$ is also visible on the PAA-GEM measurement. The C-F bond stretching at 1400-1000 $cm^{-1}$ from gemcitabine is also shown on the PAA-GEM nanoparticle. The formation of the amide bond was found in spectrum as well as the C-F band, confirming the conjugation between PAA and GEM.

## Encapsulation Efficiency and loading capacity:

The encapsulation efficiency (EE) of the particle was determined through indirect analysis of gemcitabine via investigation of the supernatant of the centrifuged sample. Using the previously mentioned equations (1) and (2), the EE and LC were determined to be 29.29 ± 1.66 and 9.44%, respectively.

## Nanoparticle Stability

The stability of the PAA-GEM nanoparticles were studied over several days at different pH environments, from pH 4 to 7.4. Table 3 demonstrates day one of investigation, here as the pH of the nanoparticles increased the size of the nanoparticles increased as well in the pH 4-6 solutions in sodium acetate buffer. The surface charge of particles in the pH 4-6 solutions became increasingly negative as the pH increased. Interestingly, the size of the pH 6 solution was larger than the pH 7.4 as well as the surface charge of the pH 6 solution was more negative then the pH 7.4 solution. Figures 4 a and 4 b, demonstrate a prolonged study of seven days to observe the surface charge and size, respectively. Over time, the size of the nanoparticles increased for all pH solutions. As for the surface charge of the nanoparticles they remained within the same range for the entirety of the analysis. However, the pH 4 solution was resistant to change throughout and retained a similar surface charge and size during the prolonged study.

## In Vitro Drug Release

The release profile of free GEM and PAA-GEM nanoparticles was studied for 96 hours (5, 10, 15, 30, 45 minutes, 1, 1.5, 2, 3, 6, 12, 24, 48, 72 and 96 hours). Figure 5 demonstrates the releasing profile of free GEM and PAA-GEM nanoparticles. Free GEM was released at a

continuous rate with 12.92% released in the first 5 minutes and 95.84% after 6 hours. PAA-GEM nanoparticles released 1.00% of GEM after 2 hours and at 96 hours, only 6.79% of the total GEM was released.

## Cytotoxicity Study

Cell viability studies were performed to determine the efficiency of the PAA-GEM nanoparticles against free GEM. As shown in figure 6, free GEM, PAA and PAA-GEM nanoparticles were compared at different concentrations and time for their cytotoxicity. For the concentrations of 0.01 μM and 0.1 μM no noticeable differences were observed between the controls and the nanoparticles for the entire 96 hours. At 24 hours of incubation no significant differences were seen between the PAA-GEM nanoparticles and free GEM for all the concentrations studied. After 48 hours cell viability decreased for 5 μM and 10 μM concentrations for the cell colonies treated with free GEM to 73.7 ± 2.8% and 61.7 ± 4.9%, respectively. At 72 hours free GEM continued to decrease the cell viability for 5 μM and 10 μM to 54.7 ± 2.6 % and 49.5 ± 2.5%, respectively. In addition, the cell viability for the PAA-GEM nanoparticles also begins to decrease at 72 hours for the 10 μM concentration to 67.2 ± 4.7%. However, there were still more cells viable in the PAA-GEM cell colonies compared to the free GEM colonies. At 96 hours the cell viability for PAA-GEM nanoparticles was similar to the cell viability of free GEM for both the 5 μM and 10 μM concentrations. The cells treated with free GEM had cell viability at 56.0 ± 4.6% and 42.1 ± 1.6% for the 5 μM and 10 μM, respectively. The cell viability at 96 hours for the PAA-GEM nanoparticles was 61.5 ± 3.1 and 44.3 ± 3.7% at 96 hours, respectively.

## Cell Uptake Kinetics

In order to determine the uptake of the nanoparticles within the cell a kinetic study was designed to observe the amount of fluorescence within cells at various time intervals. Rhodamine G6 nanoparticles were incubated with PANC-1 cells and the fluorescence at different times was determined. As shown in figure 7, the kinetic study reveals that the fluorescens intensity increases from 30 minutes to 2 hours and reaches equilibrium at 2-5 hours.

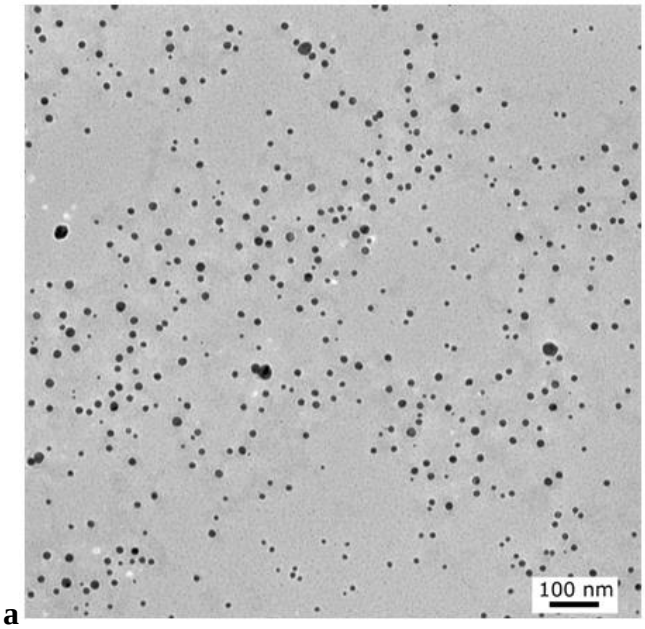


**a**

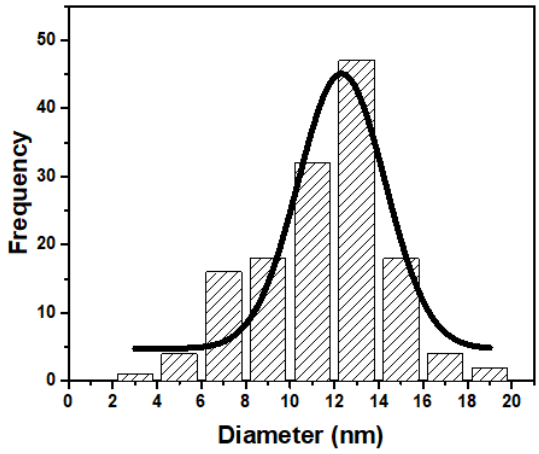


**b**

Figure 2- Nanoparticle size. Transmission electron microscopy (TEM) of PAA-GEM NP (a); size distribution histogram of the nanoparticles from TEM image (b)

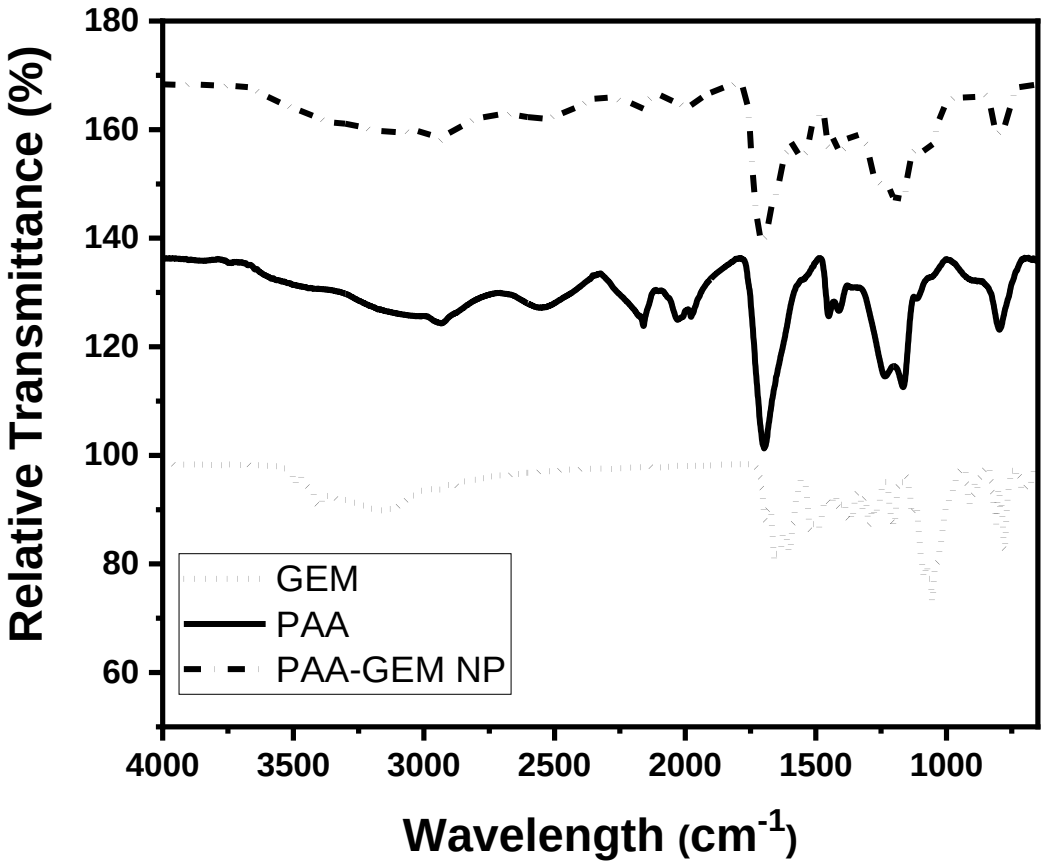


Figure 3 FTIR spectra of GEM, PAA and PAA-GEM

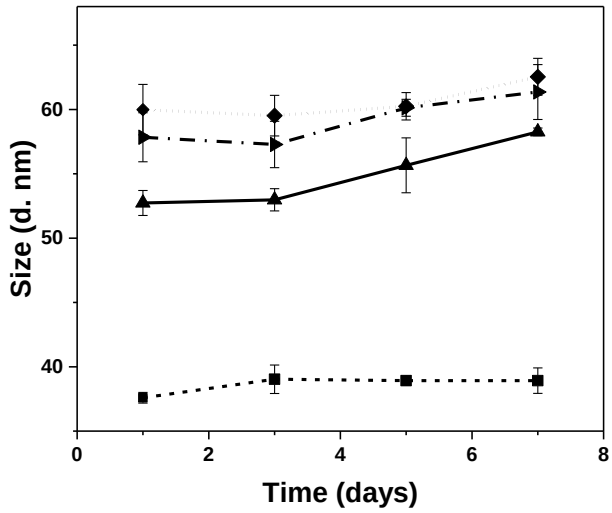


**a**

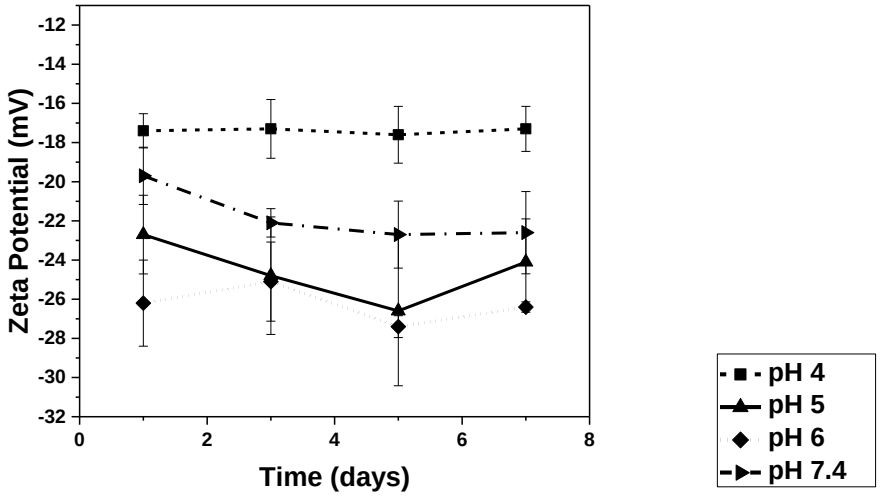


**b**

Figure 4 Nanoparticle Stability: The sizes of PAA-GEM NP at different pH (a). Surface charge of PAA-GEM NP at different pH (b)

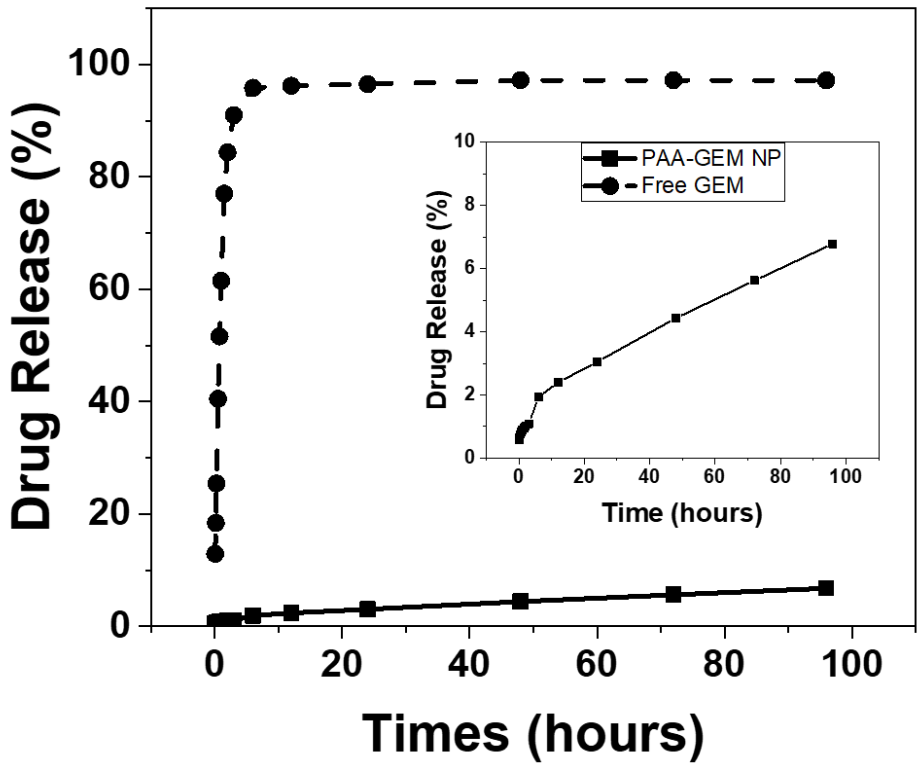


Figure 5 Drug release profile of free GEM and PAA-GEM NP

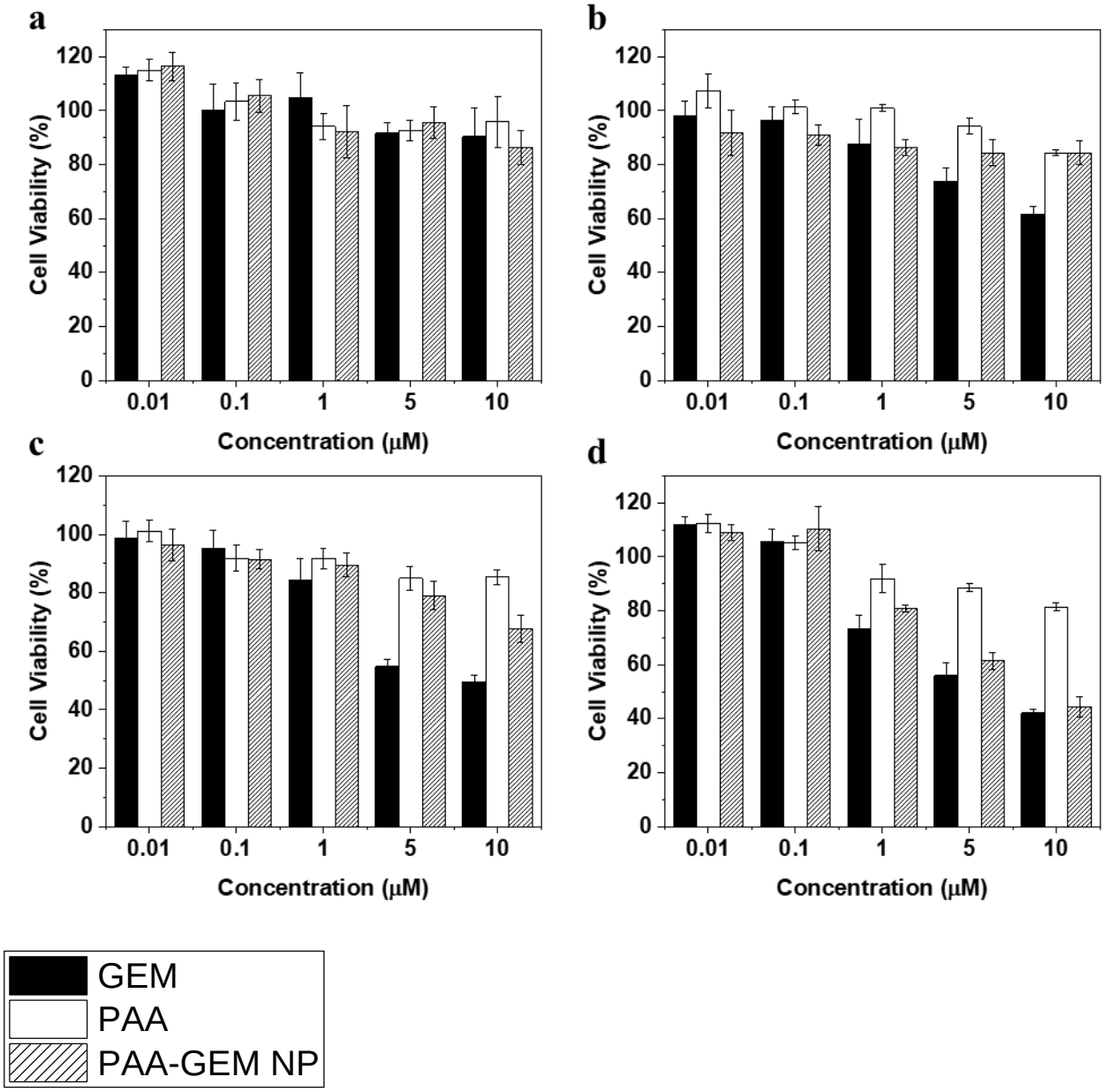


Figure 6 Cell viability study: PANC-1 cells treated with various concentrations of GEM, PAA and PAA-GEM NP at various time intervals 24 hours (a); 48 hours (b); 72 hours (c); and 96 hours (d).

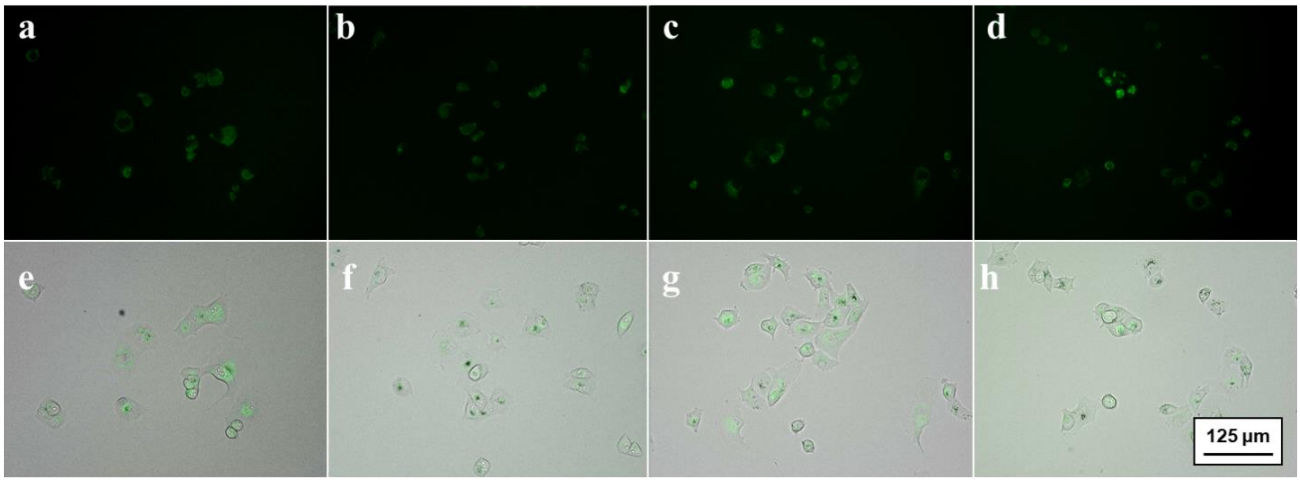


Figure 7 Cell uptake kinetics: Fluorescence images and fluorescence/bright-field overlay images of PANC-1 cells incubated with PAA-GEM-RG6 nanoparticles at 30 min (a, e); 2h(b, f); 4h (c, g); and 6h (d, h).

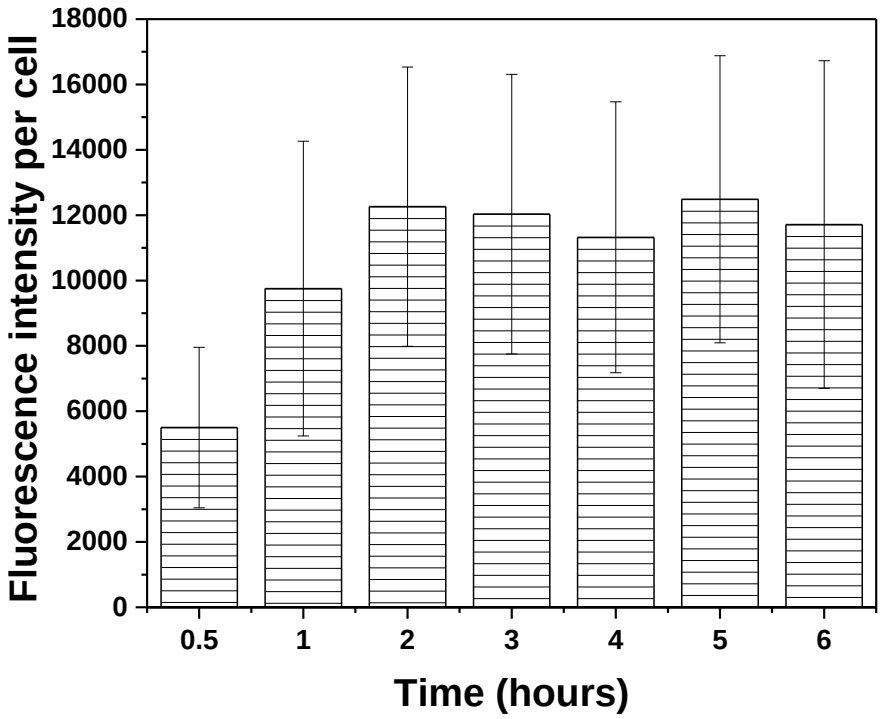


Figure 8 Cell uptake kinetics: Cellular uptake of PAA-GEM-RG6 NP into PANC-1 cells. Quantitative analysis of cell fluorescence at various time intervals based on confocal images

Table 1 Effects of PAA:GEM ratio to nanoparticles size, PDI and zeta potential. 8:1 and 16:1 solutions failed to make particles

| PAA:GEM (mol:mol) | Size ± sd. (d. nm) | PDI (± sd.) | Zeta Potential (mV) |
|---|---|---|---|
| 2:1 | 3574 ± 493.1 | 0.264 ± 0.133 | -23.0 ± 4.42 |
| 4:1 | 69.62 ± 0.419 | 0.211 ± 0.014 | -16.8 ± 1.36 |
| 8:1 | - | - | - |

Table 2 Effects of EDC to gemcitabine ratio to nanoparticle size most effective at pH 4

| PAA:GEM:EDC (mol:mol:mol) | Size ± sd. (d. nm) | PDI (± sd.) | Zeta Potential (mV) |
|---|---|---|---|
| 4:1:2 | 69.62 ± 0.419 | 0.211 ± 0.014 | -16.8 ± 1.36 |
| 4:1:4 | 2781 ± 0.986 | 0.986 ± 0.024 | -17 ± 1.52 |
| 4:1:8 | 4347± 809.7 | 1.000 ± 0 | -30.8 ± 5.77 |
| 8:1:4 | 43.38 ± 7.635 | 0.401 ± 0.125 | -16.5 ± 0.529 |
| 8:1:8 | 28.74 ± 0.127 | 0.229 ± 0.006 | -15.8 ± 0.802 |

Table 3 Change in size of PAA:GEM nanoparticles with PAA:GEM-RG6 in PBS

| | **Size ± sd. (d. nm)** | **PDI (± sd.)** | **Zeta Potential (mV)** |
|---|---|---|---|
| PAA:GEM | 63.99 ± | 0.114 ± | -23.3 ± |
| PAA:GEM:RG6 | 59.96 ± 0.926 | 0.258 ± 0.029 | -23.022 ± 1.23 |

Table 4 Effects of pH for PAA:GEM nanoparticles

| **pH** | **Size ± sd. (d. nm)** | **PDI (± sd.)** | **Zeta Potential (mV)** |
|---|---|---|---|
| 4 | 37.59 ± 0.416 | 0.142 ± 0.008 | -17.4 ± 0.874 |
| 5 | 52.73 ± 0.971 | 0.242 ± 0.024 | -22.7 ± 2.01 |
| 6 | 59.99 ± 1.960 | 0.169 ± 0.009 | -26.2 ±2.2 |
| 7.4 | 57.84 ± 1.909 | 0.169 ± 0.015 | -19.7 ± 1.46 |

# CHAPTER FOUR: DISCUSSION

The fabrication of the nanoparticles was achieved by carbodiimide chemistry between the carboxylic acids of PAA and the amine groups of gemcitabine. Several studies have shown the formation of an amide bond from the amine group of gemcitabine using EDC for the use in nanoparticles. [49] [46] However, no reported study has shown the formation of nanoparticles with the introduction of EDC to GEM and its conjugated polymer. Here, the formation of the nanoparticles is driven by the hydrophobic region of GEM collecting in the core of the nanoparticle. Figure 1b, illustrates the difluoro group within GEM, that results in the hydrophobicity of gemcitabine from the C-F bond.[50] [51] The polyelectrolyte PAA then forms an external shell.

Different PAA:GEM ratios were investigated for the fabrication of nanoparticles. For all ratios, the pH of the solutions was adjusted to 4 with 1M NaOH, as the pKa of gemcitabine and PAA are 3.6 and 4.2, respectively.[11, 52]. A pH between the pKa of both materials allows for the most optimal electrostatic interaction between the positively charged amine of gemcitabine and the negatively charged carboxylic acid of PAA. The amount of EDC added to each solution was in excess to GEM for a 2:1 molar ratio of EDC:GEM. The difference in size between the 2:1:2 and 4:1:2 (PAA:GEM:EDC) may have been the result of the amount of GEM collecting in the core of the nanoparticle that increased the overall size. As the particle is larger and at the same pH there are more external PAA units in the 2:1:2 ratio compared to the 4:1:2 ratio (PAA:GEM:EDC) nanoparticles, resulting in a more negatively charged particles.

The effects of EDC to GEM was then investigated with the 4:1 and the 8:1 PAA:GEM ratio solutions. In the 4:1 PAA:GEM solutions with the increase of EDC the solution became cloudier and formed micron sized particles, this was the result of a higher collection of GEM in the core

and higher coupling activity of EDC resulting in loosely formed large particles. The difference in size between the 8:1 and 4:1 nanoparticles may be a result of higher conjugation of GEM in the 8:1 EDC:GEM samples, resulting in smaller particles as there is a more concentrated hydrophobic core. As previously seen, the larger particles have a more negative zeta potential as there are more exterior units of PAA. As a result of the smaller size and low PDI the 8:1:8 PAA:GEM:EDC nanoparticle was chosen for further studies. A PDI below 0.3 indicates a monodisperse collection of nanoparticles that may be used for pharmaceutical applications.[53]

The discrepancy in size between TEM and DLS measurements are a result of the TEM measurement being investigated in a dried vacuumed state while DLS measurements were taken while in the hydrodynamic state resulting in sizes of 12.32 ± 1.96 nm and 57.84 ± 1.90 nm in PBS, respectively.

The attachment of RG6 is coupled through a EDC reaction of the secondary amine of RG6 and the carboxylic acid of PAA. RG6 is slightly hydrophobic due to the aromatic rings, resulting in the coupling of RG6 to the nanoparticle to occur within the internal pockets of the hydrogel nanoparticle. The attachment of RG6 demonstrated a slight change in size of the nanoparticles increasing from 57.84 ± 1.90 nm to 59.96 ± 0.926 nm, when compared to the undecorated PAA-GEM nanoparticle. The decrease in surface charge may have been a result of the increase in size of the nanoparticle as there are more external PAA groups to contribute to the surface charge.

The conjugation between PAA and GEM were confirmed through FT-IR, the formation of an amide bond is demonstrated in the PAA-GEM samples with the C=O stretching at 1680-1700 $cm^{-1}$ as the amide I band. The amide II band at 1550-1510 $cm^{-1}$ is also visible on the PAA-GEM measurement. The amine stretching from GEM at 3500-3300 $cm^{-1}$ is not visible in the PAA-GEM

nanoparticle, due to reaction of the amine. The C-F bond at 1400-1000 $cm^{-1}$ from GEM is also shown on the PAA-GEM nanoparticle. As the formation of the amide bond was found within the PAA-GEM spectrum as well as the C-F band, the conjugation between PAA and gemcitabine was confirmed.

The encapsulation efficiency of the nanoparticles was demonstrated to be 29 ± 1.66% compared to other studies where the encapsulation of GEM has been reported in the range 2-70%.[43, 44, 54-56] The loading capacity of GEM recovered was 9.44%, other studies have demonstrated loading capacities of 0.02-43%.[44, 55, 57] The encapsulation efficiency and loading capacity obtained in this study are within the range of previously reported values.

During the investigation of the stability of the nanoparticles in different pH environments it was observed that the nanoparticle sizes increased with increasing pH. This is a result of the nature of a hydrogel nanoparticle; as the pH of the solution increases above the pKa of PAA the individual carboxylic acid groups begin to deprotonate and ionize. The electrostatic repulsion between the PAA-GEM nanoparticle results in the swelling of the nanoparticle, which causes the increase in the size. The increasing ionization also results in more negatively charged surface of the nanoparticle. Comparing the pH 6 and pH 7.4 solutions, the results do not follow the trend in increasing size as the pH nanoparticles were resuspended in PBS. The particles may be smaller as there are more free ions in the PBS solution resulting in a hypertonic solution decreasing the size of the nanoparticles. Additionally, PBS contains divalent ions such as calcium and magnesium, bridging of PAA molecules has been demonstrated between divalent ions such as calcium.[58] This bridging effect as well as the hypertonic solution of PBS compared to sodium acetate buffer resulted in the smaller size and less negative surface of the pH 7.4 resuspended nanoparticles.

During the in vitro release of PAA-GEM nanoparticles only 6.79% of internalized GEM was released after 96 hours. Interestingly, the release of GEM may have occurred from unbound GEM located in the internal pockets of the hydrogel nanoparticle. The remaining GEM is conjugated via amide bond in the core of the nanoparticle. Other drug delivery studies have shown an initial burst release from the first few hours where up to 45-70% of the drug can be released.[59-61] An initial burst release was not demonstrated in the PAA-GEM nanoparticle indicating a slow and sustained release.

PANC-1 cells, a GEM resistant cell line was used to determine the efficiency of the nanoparticles.[62] Concentrations between the range of 0.01 µM -10 µM were selected to determine cell toxicity as the $IC_{50}$ of GEM to various PDAC cell lines fall with this range. The $IC_{50}$ value for GEM on PANC-1 cells is 9.5 µM.[63] From the cytotoxicity study PAA-GEM nanoparticles did not show any signs of cell toxicity within the first 48 hours comparted to the free GEM. However, at 96 hours of incubation in the PANC-1 cells the 10 µM PAA-GEM nanoparticles demonstrated similar cytotoxic efficacy as the free GEM with cell viability at 44.3 ± 3.7% and 42.0 ± 1.6, respectively. This demonstrated full cytotoxic effects at 96 hour as the $IC_{50}$ of GEM is 9.5 µM for PANC-1 cells and ~40% of cells were still viable. In agreement with the in-vitro release study PAA-GEM nanoparticles reveal a slow release of GEM as shown here. However, the degradation of PAA-GEM NP needed further investigation.

Cell Uptake studies were preformed to establish if the PAA-GEM nanoparticles were broken inside the cell or by enzymes in the free growth media. The decorated PAA-GEM-RG6 nanoparticles were incubated in PANC-1 cells. From the results it is seen that the nanoparticles are internalized as early as 30 minutes and gradually increase until full uptake at 2 hours. The

uptake of nanoparticles regulates and reaches equilibrium at 2-5 hours. Similar results have been seen with other polymer nanoparticles where internalization began within 30 minutes and were fully internalized at 2 hours.[40, 64, 65] This data confirms that the degradation of the nanoparticles occurs after the uptake of the nanoparticles inside the cell.

# CHAPTER FIVE:CONCLUSION

The main objective of this study was to fabricate a nanoparticle with internal gemcitabine core in order to protect the drug from degradation and protect the subject from cytotoxic effects of gemcitabine. Here we were able to create a facile fabrication method for nanoparticles using small hydrophobic molecules and polyelectrolytes. In our study GEM served as our small hydrophobic molecule and PAA our polyelectrolyte, after conjugation of GEM on to PAA the nanoparticles formed. The size of the nanoparticles were investigated to be 57.84 ± 1.909 nm in PBS and with a PDI of 0.169 ± 0.015 in PBS, demonstrating a nanoparticle that can be used for clinical use. The stability of the nanoparticles were investigated as well, the studies demonstrated that the nanoparticle had minimal changes in various pH conditions over 7 days. The cytotoxic efficiency demonstrated a slow release of the drug and overall comparable to free gem after 96 hours. Uptake study of the nanoparticles into cells was examined as well and full uptake of the nanoparticles occurred after 2 hours. Overall, we fabricated a nanoparticle that can be used for treatment of pancreatic cancer.

Future outlooks include the addition of targeting enzymes to the PAA-GEM nanoparticle to allow for specific cell type targeting. Further modulations can be used to decorate the nanoparticles including the attachment of other molecules for in vivo bioimaging. The facile fabrication of the PAA-GEM nanoparticles yielded monodispersed nanoparticles and the methods can be transferred to create other nanoparticles with hydrophobic molecules and polyelectrolyte. The method of fabrication demonstrated here is currently under investigation for the fabrication of PAA-Guanosine-Cerium nanoparticles, for the scavenging of reactive oxygen species. In

conclusion is that we were able to demonstrate a novel fabrication method of nanoparticles using only electrolytes and hydrophobic molecules.

# LIST OF REFERENCES


1. Iravani, S., Bacteria in Nanoparticle Synthesis: Current Status and Future Prospects. *International Scholarly Research Notices* **2014,** *2014*, 1-18.

2. Pantidos, N., Biological Synthesis of Metallic Nanoparticles by Bacteria, Fungi and Plants. *Journal of Nanomedicine & Nanotechnology* **2014,** *05* (05).

3. Hamidi, M.; Azadi, A.; Rafiei, P., Hydrogel nanoparticles in drug delivery. *Advanced Drug Delivery Reviews* **2008,** *60* (15), 1638-1649.

4. Jeevanandam, J.; Barhoum, A.; Chan, Y. S.; Dufresne, A.; Danquah, M. K., Review on nanoparticles and nanostructured materials: history, sources, toxicity and regulations. *Beilstein J Nanotechnol* **2018,** *9*, 1050-1074.

5. Durán, N.; Nakazato, G.; Seabra, A. B., Antimicrobial activity of biogenic silver nanoparticles, and silver chloride nanoparticles: an overview and comments. *Applied Microbiology and Biotechnology* **2016,** *100* (15), 6555-6570.

6. Martins, M.; Mourato, C.; Sanches, S.; Noronha, J. P.; Crespo, M. T. B.; Pereira, I. A. C., Biogenic platinum and palladium nanoparticles as new catalysts for the removal of pharmaceutical compounds. *Water Research* **2017,** *108*, 160-168.

7. Wang, J.; Polleux, J.; Lim, J.; Dunn, B., Pseudocapacitive contributions to electrochemical energy storage in TiO 2 (anatase) nanoparticles. *Journal of Physical Chemistry C* **2007,** *111* (40), 14925-14931.

8. Wadhwani, S. A.; Shedbalkar, U. U.; Singh, R.; Vashisth, P.; Pruthi, V.; Chopade, B. A., Kinetics of Synthesis of Gold Nanoparticles by Acinetobacter sp. SW30 Isolated from Environment. *Indian Journal of Microbiology* **2016,** *56* (4), 439-444.

9. Medintz, I. L.; Uyeda, H. T.; Goldman, E. R.; Mattoussi, H., Quantum dot bioconjugates for imaging, labelling and sensing. *Nature Materials* **2005,** *4* (6), 435-446.

10. Chen, D.-W.; Cheng, L.; Huang, F.; Cheng, L.; Zhu, Y.; Hu, Q.; Li, L.; Wei, L., GE11-modified liposomes for non-small cell lung cancer targeting: preparation, ex vitro and in vivo evaluation. *International Journal of Nanomedicine* **2014,** *9* (1), 921-921.

11. Wu, Y.; Wu, J.; Cao, J.; Zhang, Y.; Xu, Z.; Qin, X.; Wang, W.; Yuan, Z., Facile fabrication of poly(acrylic acid) coated chitosan nanoparticles with improved stability in biological environments. *European Journal of Pharmaceutics and Biopharmaceutics* **2017,** *112,* 148-154.

12. Crucho, C. I. C.; Barros, M. T., Polymeric nanoparticles: A study on the preparation variables and characterization methods. *Materials Science and Engineering: C* **2017,** *80,* 771-784.

13. Elsabahy, M.; Wooley, K. L., Design of polymeric nanoparticles for biomedical delivery applications. *Chemical Society reviews* **2012,** *41* (7), 2545-2561.

14. Kumari, A.; Yadav, S. K.; Yadav, S. C., Biodegradable polymeric nanoparticles based drug delivery systems. *Colloids and Surfaces B: Biointerfaces* **2010,** *75* (1), 1-18.

15. Annabi, N.; Tamayol, A.; Uquillas, J. A.; Akbari, M.; Bertassoni, L. E.; Cha, C.; Camci-Unal, G.; Dokmeci, M. R.; Peppas, N. A.; Khademhosseini, A., 25th anniversary article: Rational design and applications of hydrogels in regenerative medicine. *Advanced Materials* **2014,** *26* (1), 85-124.

16. Ahmed, E. M., Hydrogel: Preparation, characterization, and applications: A review. *Journal of Advanced Research* **2015,** *6* (2), 105-121.

17. Thoniyot, P.; Tan, M. J.; Karim, A. A.; Young, D. J.; Loh, X. J., Nanoparticle–Hydrogel Composites: Concept, Design, and Applications of These Promising, Multi-Functional Materials. *Advanced Science* **2015,** *2* (1-2), 1-13.

18. Caló, E.; Khutoryanskiy, V. V., Biomedical applications of hydrogels: A review of patents and commercial products. *European Polymer Journal* **2015,** *65*, 252-267.

19. Vlierberghe, S. V.; Dubruel, P.; Schacht, E., Biopolymer-Based Hydrogels As Scaffolds for Tissue Engineering Applications : A Review. **2011**, 1387-1408.

20. Heo, D. N.; Castro, N. J.; Lee, S. J.; Noh, H.; Zhu, W.; Zhang, L. G., Enhanced bone tissue regeneration using a 3D printed microstructure incorporated with a hybrid nano hydrogel. *Nanoscale* **2017,** *9* (16), 5055-5062.

21. Swarnalatha, S.; Gopi, R.; Ganesh Kumar, A.; Selvi, P. K.; Sekaran, G., A novel amphiphilic nano hydrogel using ketene based polyester with polyacrylamide for controlled drug delivery system. *Journal of Materials Science: Materials in Medicine* **2008,** *19* (9), 3005-3014.

22. Qu, J.; Zhao, X.; Liang, Y.; Xu, Y.; Ma, P. X.; Guo, B., Degradable conductive injectable hydrogels as novel antibacterial, anti-oxidant wound dressings for wound healing. *Chemical Engineering Journal* **2019,** *362* , 548-560.

23. Christensen, L.; Breiting, V.; Janssen, M.; Vuust, J.; Hogdall, E., Adverse Reactions to Injectable Soft Tissue Permanent Fillers. *Aesthetic Plastic Surgery* **2005,** *29* (1), 34-48.

24. Brahim, S.; Narinesingh, D.; Guiseppi-Elie, A., Polypyrrole-hydrogel composites for the construction of clinically important biosensors. *Biosensors and Bioelectronics* **2002,** *17* (1), 53-59.

25. Gonçalves, C.; Pereira, P.; Gama, M., Self-assembled hydrogel nanoparticles for drug delivery applications. *Materials* **2010,** *3* (2), 1420-1460.

26. Genta, I.; Chiesa, E.; Colzani, B.; Modena, T.; Conti, B.; Dorati, R., GE11 peptide as an active targeting agent in antitumor therapy: A minireview. *Pharmaceutics* **2018,** *10* (1).

27. Maxwell, T.; Banu, T.; Price, E.; Tharkur, J.; Campos, M.; Gesquiere, A.; Santra, S., Non-Cytotoxic Quantum Dot–Chitosan Nanogel Biosensing Probe for Potential Cancer Targeting Agent. *Nanomaterials* **2015,** *5* (4), 2359-2379.

28. Malhotra, A.; Zhang, X.; Turkson, J.; Santra, S., Buffer-stable chitosan-polyglutamic acid hybrid nanoparticles for biomedical applications. *Macromolecular Bioscience* **2013,** *13* (5), 603-613.

29. Kurtoglu, Y. E.; Mishra, M. K.; Kannan, S.; Kannan, R. M., Drug release characteristics of PAMAM dendrimer-drug conjugates with different linkers. *International Journal of Pharmaceutics* **2010,** *384* (1-2), 189-194.

30. Parsian, M.; Unsoy, G.; Mutlu, P.; Yalcin, S.; Tezcaner, A.; Gunduz, U., Loading of Gemcitabine on chitosan magnetic nanoparticles increases the anti-cancer efficacy of the drug. *European Journal of Pharmacology* **2016,** *784*, 121-128.

31. Tallury, P.; Kar, S.; Bamrungsap, S.; Huang, Y.-F.; Tan, W.; Santra, S., Ultra-small water-dispersible fluorescent chitosan nanoparticles: synthesis, characterization and specific targeting. *Chemical Communications* **2009,** (17), 2347-2349.

32. Maibaum, L.; Dinner, A. R.; Chandler, D., Micelle Formation and the Hydrophobic Effect. *The Journal of Physical Chemistry B* **2004,** *108* (21), 6778-6781.

33. Tanford, C., Theory of micelle formation in aqueous solutions. *The Journal of Physical Chemistry* **1974,** *78* (24), 2469-2479.

34. Wei, H.; Zhang, X.-Z.; Zhou, Y.; Cheng, S.-X.; Zhuo, R.-X., Self-assembled thermoresponsive micelles of poly(N-isopropylacrylamide-b-methyl methacrylate). *Biomaterials* **2006,** *27* (9), 2028-2034.

35. Abbasi, E.; Aval, S. F.; Akbarzadeh, A.; Milani, M.; Nasrabadi, H. T.; Joo, S. W.; Hanifehpour, Y.; Nejati-Koshki, K.; Pashaei-Asl, R., Dendrimers: synthesis, applications, and properties. *Nanoscale Res Lett* **2014,** *9* (1), 247-247.

36. Grayson, S. M.; Fréchet, J. M. J., Convergent Dendrons and Dendrimers: from Synthesis to Applications. *Chemical Reviews* **2001,** *101* (12), 3819-3868.

37. Miladi, K.; Sfar, S.; Fessi, H.; Elaissari, A., Nanoprecipitation Process: From Particle Preparation to In Vivo Applications. In *Polymer Nanoparticles for Nanomedicines: A Guide for their Design, Preparation and Development*, Vauthier, C.; Ponchel, G., Eds. Springer International Publishing: Cham, 2016; pp 17-53.

38. Martínez Rivas, C. J.; Tarhini, M.; Badri, W.; Miladi, K.; Greige-Gerges, H.; Nazari, Q. A.; Galindo Rodríguez, S. A.; Román, R. Á.; Fessi, H.; Elaissari, A., Nanoprecipitation process: From encapsulation to drug delivery. *International Journal of Pharmaceutics* **2017,** *532* (1), 66-81.

39. Yadav, K. S.; Sawant, K. K., Modified nanoprecipitation method for preparation of cytarabine-loaded PLGA nanoparticles. *AAPS PharmSciTech* **2010,** *11* (3), 1456-1465.

40. Colzani, B.; Speranza, G.; Dorati, R.; Conti, B.; Modena, T.; Bruni, G.; Zagato, E.; Vermeulen, L.; Dakwar, G. R.; Braeckmans, K.; Genta, I., Design of smart GE11-PLGA/PEG-PLGA blend nanoparticulate platforms for parenteral administration of hydrophilic macromolecular drugs: synthesis, preparation and in vitro/ex vivo characterization. *International Journal of Pharmaceutics* **2016,** *511* (2), 1112-1123.

41. Manzur, A.; Oluwasanmi, A.; Moss, D.; Curtis, A.; Hoskins, C., Nanotechnologies in pancreatic cancer therapy. *Pharmaceutics* **2017,** *9* (4).

42. De Sousa Cavalcante, L.; Monteiro, G., Gemcitabine: Metabolism and molecular mechanisms of action, sensitivity and chemoresistance in pancreatic cancer. *European Journal of Pharmacology* **2014,** *741*, 8-16.

43. Arya, G.; Vandana, M.; Acharya, S.; Sahoo, S. K., Enhanced antiproliferative activity of Herceptin (HER2)-conjugated gemcitabine-loaded chitosan nanoparticle in pancreatic cancer therapy. *Nanomedicine: Nanotechnology, Biology, and Medicine* **2011,** *7* (6), 859-870.

44. Arias, J. L.; Reddy, L. H.; Couvreur, P., Superior preclinical efficacy of gemcitabine developed as chitosan nanoparticulate system. *Biomacromolecules* **2011,** *12* (1), 97-104.

45. Sandoval, M. A.; Sloat, B. R.; Lansakara-P, D. S. P.; Kumar, A.; Rodriguez, B. L.; Kiguchi, K.; Digiovanni, J.; Cui, Z., EGFR-targeted stearoyl gemcitabine nanoparticles show enhanced anti-tumor activity. *Journal of Controlled Release* **2012,** *157* (2), 287-296.

46. Mu, Q.; Lin, G.; Patton, V. K.; Wang, K.; Press, O. W.; Zhang, M., Gemcitabine and Chlorotoxin Conjugated Iron Oxide Nanoparticles for Glioblastoma Therapy. 2016; Vol. 4, pp 32-36.

47. De Giglio, E.; Cafagna, D.; Ricci, M. A.; Sabbatini, L.; Cometa, S.; Ferretti, C.; Mattioli-Belmonte, M., Biocompatibility of Poly(Acrylic Acid) Thin Coatings Electro-synthesized onto TiAlV-based Implants. *Journal of Bioactive and Compatible Polymers* **2010,** *25* (4), 374-391.

48. Bai, M.; Wilske, B.; Buegger, F.; Esperschütz, J.; Bach, M.; Frede, H.-G.; Breuer, L., Relevance of nonfunctional linear polyacrylic acid for the biodegradation of superabsorbent polymer in soils. *Environmental Science and Pollution Research* **2015,** *22* (7), 5444-5452.

49. Santiago, T.; Espinal, R.; Hepel, M., Surface-enhanced Raman scattering investigation of targeted delivery and controlled release of gemcitabine. *International Journal of Nanomedicine* **2017,** *12*, 7763-7776.

50. Biffinger, J. C.; Kim, H. W.; DiMagno, S. G., The polar hydrophobicity of fluorinated compounds. *ChemBioChem* **2004,** *5* (5), 622-627.

51. Dalvi, V. H.; Rossky, P. J., Molecular origins of fluorocarbon hydrophobicity. *Proceedings of the National Academy of Sciences* **2010,** *107* (31), 13603-13607.

52. Xu, H.; Paxton, J.; Lim, J.; Li, Y.; Zhang, W.; Duxfield, L.; Wu, Z., Development of high-content gemcitabine PEGylated liposomes and their cytotoxicity on drug-resistant pancreatic tumour cells. *Pharmaceutical research* **2014,** *31* (10), 2583-2592.

53. Dehghankhold, M.; Mozafari, M.; Ataei, S.; Danaei, M.; Hasanzadeh Davarani, F.; Khorasani, S.; Javanmard, R.; Dokhani, A., Impact of Particle Size and Polydispersity Index on the Clinical Applications of Lipidic Nanocarrier Systems. *Pharmaceutics* **2018,** *10* (2), 57-57.

54. Yalcin, T. E.; Ilbasmis-Tamer, S.; Ibisoglu, B.; Özdemir, A.; Ark, M.; Takka, S., Gemcitabine hydrochloride-loaded liposomes and nanoparticles: comparison of encapsulation efficiency, drug release, particle size, and cytotoxicity. *Pharmaceutical Development and Technology* **2018,** *23* (1), 76-86.

55. Hosseinzadeh, A. D. O., Chitosan – Pluronic nanoparticles as oral delivery of anticancer gemcitabine : preparation and in vitro study. *International Journal of Nanomedicine* **2012**, 1851-1863.

56. Derakhshandeh, K.; Fathi, S., Role of chitosan nanoparticles in the oral absorption of Gemcitabine. *International Journal of Pharmaceutics* **2012,** *437* (1-2), 172-177.

57. Razzazan, A.; Atyabi, F.; Kazemi, B.; Dinarvand, R., In vivo drug delivery of gemcitabine with PEGylated single-walled carbon nanotubes. *Materials Science and Engineering: C* **2016,** *62*, 614-625.

58. Nap, R. J.; Park, S. H.; Szleifer, I., Competitive calcium ion binding to end-tethered weak polyelectrolytes. *Soft Matter* **2018,** *14* (12), 2365-2378.

59. Fonte, P.; Soares, S.; Costa, A.; Andrade, J. C.; Seabra, V.; Reis, S.; Sarmento, B., Effect of cryoprotectants on the porosity and stability of insulin-loaded PLGA nanoparticles after freeze-drying. *Biomatter* **2012,** *2* (4), 329-339.

60. Gan, Q.; Wang, T., Chitosan nanoparticle as protein delivery carrier-Systematic examination of fabrication conditions for efficient loading and release. *Colloids and Surfaces B: Biointerfaces* **2007,** *59* (1), 24-34.

61. Akbuğa, J.; Bergişadi, N., Effect of formulation variables on cis-platin loaded chitosan microsphere properties. *Journal of microencapsulation* **1999,** *16* (6), 697-703.

62. Kushwah, V.; Agrawal, A. K.; Dora, C. P.; Mallinson, D.; Lamprou, D. A.; Gupta, R. C.; Jain, S., Novel Gemcitabine Conjugated Albumin Nanoparticles: a Potential Strategy to Enhance Drug Efficacy in Pancreatic Cancer Treatment. *Pharmaceutical Research* **2017,** *34* (11), 2295-2311.

63. Awasthi, N.; Zhang, C.; Schwarz, A. M.; Hinz, S.; Wang, C.; Williams, N. S.; Schwarz, M. A.; Schwarz, R. E., Comparative benefits of Nab-paclitaxel over gemcitabine or polysorbate-based docetaxel in experimental pancreatic cancer. *Carcinogenesis* **2013,** *34* (10), 2361-2369.

64. Behzadi, S.; Serpooshan, V.; Tao, W.; Hamaly, M. A.; Alkawareek, M. Y.; Dreaden, E. C.; Brown, D.; Alkilany, A. M.; Farokhzad, O. C.; Mahmoudi, M., Cellular uptake of nanoparticles: Journey inside the cell. *Chemical Society Reviews* **2017,** *46* (14), 4218-4244.

65. Oh, N.; Park, J.-H., Endocytosis and exocytosis of nanoparticles in mammalian cells. *International journal of nanomedicine* **2014,** *9 Suppl 1* (Suppl 1), 51-63.